FRACTURE MECHANICS TESTING OF MAGNESIUM ALLOY INGOTS AND DIE CASTINGS

E. Schick and D. Regener

Institute of Materials Engineering and Materials Testing
Otto-von-Guericke-University Magdeburg
PSF 4120, 39016 Magdeburg

ABSTRACT

In the recent years has been an increase in the use of magnesium alloys, particularly for the manufacture of automotive and aerospace components. The primary benefit of magnesium alloys in structural application is their high strength to weight ratio in combination with the improved corrosion behaviour in case of the high purity alloys and the possibility to produce near net shape components with a very small wall thickness. However, an important problem for the designers is the lack of reliable data from suitable bars and real castings. Therefore, fracture mechanics investigations were made to assess the crack resistance of the magnesium alloys AZ91, AM50, AE42 from pressure die cast components, and in the case of AZ91 und AE42 from ingots, too. The specimens had been subjected to three point bending and the recorded load deflection curves were estimated.
A comparison of all the investigated alloys and conditions shows that the fracture toughness is related to the nature of the cast process and sample dependent. In case of the coarse grained AZ91 gravity cast material crack initiation occurs in the brittle intermetallic β-phase $Mg_{17}Al_{12}$, whereas the damage in the fine grained die cast materials AZ91 and AM50 starts predominantly from cavities due to shrinkage or airtrapping. The alloy AE42 proved to be more ductile both in gravity and in die cast condition. The damage process began sometimes at precititates in the grain boundaries, but in the most cases in strongly deformed solid solution matrix grains.

INTRODUCTION

The use of magnesium alloys is attributed to their high specific strength. Besides that the raw material base for magnesium is abundantly available. Therefore the potential for weight saving in automotive structures, aerospace application, computer parts, handling tools, household equipments and sporting goods is very high. Particularly the automobile industry is compelled to diminish the fuel consumption and in this way to reduce the emission of harmful agents by development lightweight constructions. But the material selection in favour of magnesium alloys requires to know the properties of different alloys and their limitations. From the application of magnesium alloys for crash sensitive components follows the necessity to characterize the different materials by mechanical parameters under static and dynamic loading and to study their deformation behaviour. An important role for crash relevant elements also plays the energy absorption described by toughness [1,2]. Therefore, the aim of this paper is to compare the alloys AZ91, AE42 (both in gravity cast and die cast condition) and the alloy AM50 in die cast condition. Impact tests and fracture mechanics tests were carried out on small specimens owing to the thin-walled die cast components. Additionally, investigations of microstructure and fracture surfaces were made for explanation of the results of mechanical testing.

MATERIAL CHARACTERIZATION AND EXPERIMENTS

Specimens were taken from ingots in case of the gravity cast (GC) alloys AZ91 and AE42 and from die cast (DC) components also for AZ91, AE42 and AM50. The chemical composition is given in Table 1. With the aim to compare all the materials with regard to their real mechanical properties investigations were carried out on specimens with the dimensions 5x10x55 mm with reference to an unnotched Charpy specimen of half thickness available from all the raw material sections. Such plates were subjected to bending and impact tests, used for hardness measurements, and microstructure investigations. Besides from these plates also small flat tensile specimens were machined with a section of ≈ 5x5 mm and a gauge length of 30 mm.
Table 2 summarizes the results of different tests.

TABLE 1
CHEMICAL COMPOSITION OF ALLOYS INVESTIGATED

Alloy/ condition	Al [%]	Zn [%]	Mn [%]	RE [%]
AZ91 (GC)	9.0	0.67	0.22	-
AZ91 (DC)	8.2	0.73	0.20	-
AE42 (GC)	4.0	0.007	0.35	2-3
AE42 (DC)	4.1	not anal.	0.19	3.2
AM50 I (DC)	4.95	0.471	0.248	-

TABLE 2
MECHANICAL PROPERTIES

Alloy/ condition	R_m [Nmm^{-2}]	A_{30} [%]	HB5/250	HV5	σ_b [Nmm^{-2}]	α [grd]	K [J]
AZ91 (GC)	115	2	66	90	208	2.6	2.7
AZ91 (DC)	180	1	72	100	270	4.6	1.4
AE42 (GC)	142	7	64	75	270	10.7	5.4
AE42 (DC)	188	4	58	64	267	12.6	6.2
AM50 I (DC)	215	2.1	64	81	350	3.2	3.5
AM50 II (DC)	125	0.8	69	92	270	2.6	1.8

The bending strength in Table 2 is calculated from the maximum load in the moment of fracture or formation of the first crack. The bending angle was actually determined after the test and is thus a measure only of the plastic deformation. For estimation of toughness all the alloys were tested at room temperature in a 15 J pendulum impact machine with an angle of impact of 90° (maximum of impact energy = 7.73 J; v = 2.73 m/s). In case of the AZ91 and AE42 gravity cast alloys and the AZ91 die cast element it was possible to manufacture real Charpy specimens. They were impact tested (with and without notch) and also used for the fracture mechanics investigations after precracking. From the other components with smaller wall thickness bending specimens were machined and partly precracked or prepared with a sawing cut by a diamond wire.

For the microstructural examination [3,4,5] the specimens were prepared by wet grinding on silicon carbide paper up to grade 2400 and by polishing with finally 1µm diamond paste. The etching solution used was 1 or 2% alcoholic nitric acid .

RESULTS AND DISCUSSION

Firstly, the results of the microstructural investigations will be discussed. Figs. 1 and 2 show the microstructure in the alloy AZ91. The microstructure reveals generally in dependence on the cooling rate. In both types of castings were found the same constituents: solid solution matrix grains surrounded by coring rims with a remarkable higher aluminium content due to the very low rate of diffusion of the Al-atoms, and the β-phase $Mg_{17}Al_{12}$. With regard to the magnification it is evident that the low solidification rate in case of the gravity cast causes the growth of large grains of 100 to 200µm in size and a certain amount of β-phase both in compact and in lamellar form, while the microstructure of the pressure die cast AZ91 with an essentially higher cooling rate is characterized by finer grains (10-20 µm) and a volume fraction of β-phase dependent on the local chemical composition and solification time [6,7].
The microstructure of the both types of the alloy AE42 is presented in Figs. 3 and 4. Rare Earth elements (RE) were added as mixed metal with a composition of 50% Ce, 25% La, 20% Nd and 3%Pr [8].

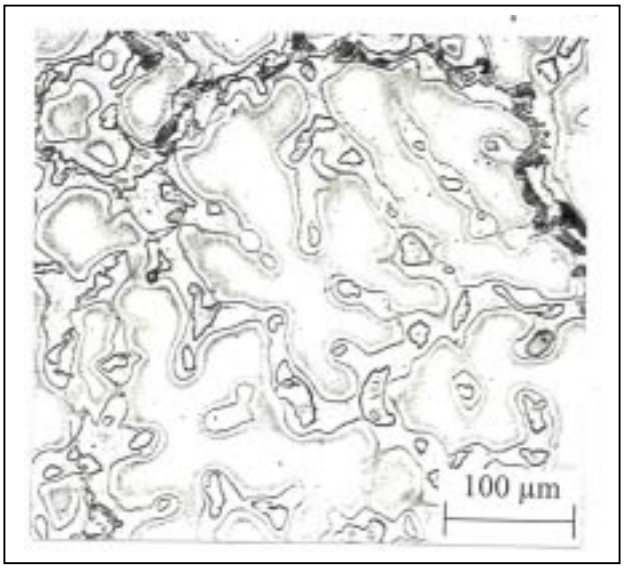

Figure 1: Microstructure of AZ91, ingot

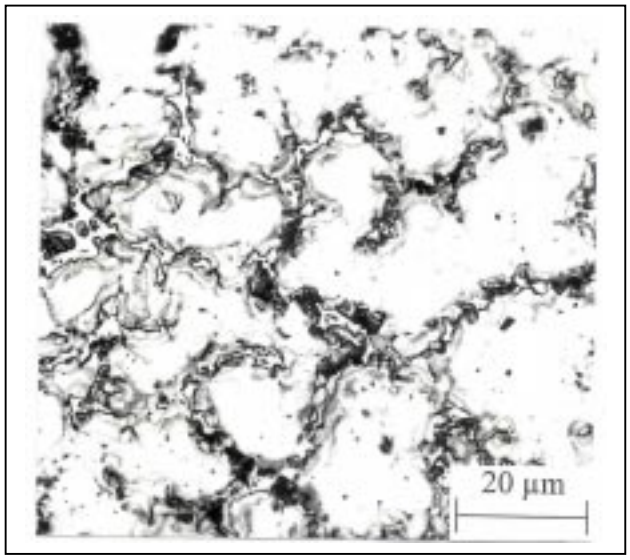

Figure 2: Microstructure of AZ91, die casting

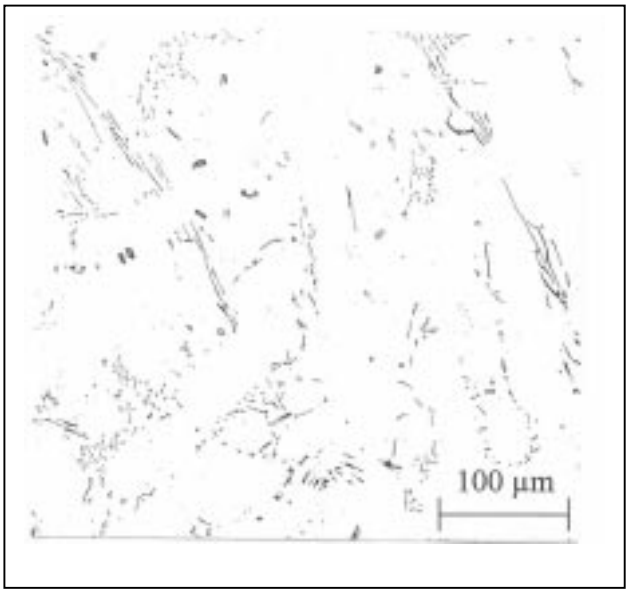

Figure 3: Microstructure of AE42, ingot

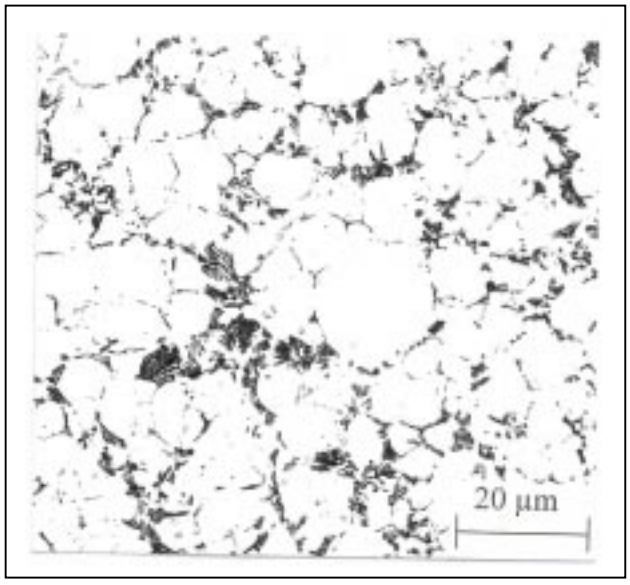

Figure 4: Microstructure of AE42, die casting

The benefit of the alloy is the retention of strength at elevated temperatures. In the ingot very large columnar macrograins were observed. Because of that no grain boundaries are visible at higher magnification. EDX-investigations reveal that the Al-content of the matrix is very low and that in agreement with the Mg-RE phase diagram no significant amounts of RE metals are dissolved in the matrix. As can be seen from Fig. 3, a great number of particles of different kinds has been precipitated.
The dark compact phase shows besides Magnesium and low Aluminium high contents of Mn and RE elements, whereas it may be assumed that the long needlelike particles are β-phase enriched with RE metals. The other lamellar or globular precipitates are eutectic phases of Al-RE- and Mg-Al-type.
In the pressure die cast condition the microstructure of the alloy AE42 appears as a fine grained α-matrix; there only exists a small fraction of with aluminium supersatured solid solutions. From additional TEM investigations [9] it was followed that the lamellar phase mixture probably consists of Al_4RE- and Mg_4Al_3-phases. At the grain boundaries small bands of β-phase can be observed, and the very small globular particles were identified as $Al_{11}RE_3$. In comparison with the gravity cast AE42 all the precipitated phases are much smaller in the pressure die cast AE42.
For the investigation of the alloy AM50 two pressure die castings were available; a steering wheel frame (I) as a crash sensitive element and a fixing element (II) without special requirements or danger potential. The addition of manganese to the Mg-Al-alloys occurs to improve the ductility of the material. The microstructure of both elements is shown in Figs. 5 and 6.

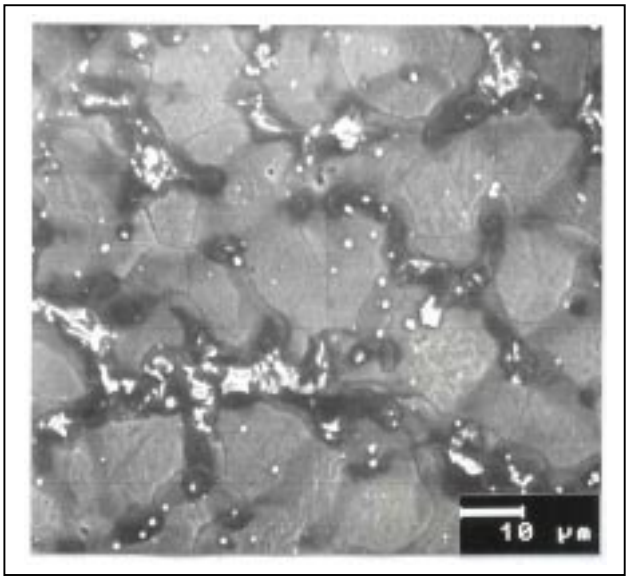

Figure 5: Microstructure of AM50 I, die casting steering wheel frame

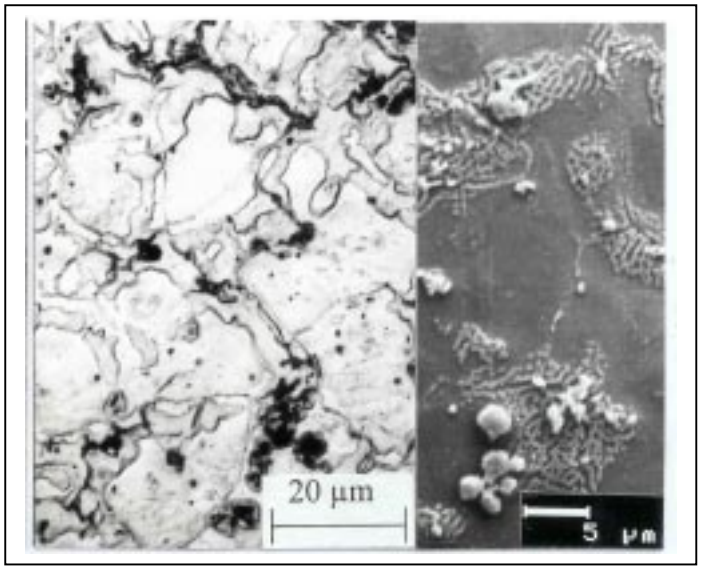

Figure 6: Microstructure of AM50 II, die casting fixing element

The solidification process of AM50 [1,6,10] is similar to that described for the alloy AZ91, but the reduced Al-content leads to a lower volume fraction of β-phase. On both images the cored matrix grains are visible and in the grain boundaries can be seen the eutectic β-phase. In the microstructure of the element II the coring was more distinct as in the steering wheel frame, also the β-content seems to be higher and in some local regions of this element the eutectic phases were found in spongelike shape (Fig. 6, right part). Besides them much microcracks and shrinkage porosity were observed**.** With regard to SEM micrographs white lumpy inclusions were found in both elements; they were identified as Al_8Mn_5-phase. The described specific microstructure in the different alloys will be correlated to the results of mechanical testing and fracture mechanics investigations.
As shown in Table 2 all the materials were characterized by mechanical parameters from industrial castings, that means these parameters are not related to defect-free material. Both the ultimate strength and the fracture elongation are to small due to local concentration of the brittle β-phase in the AZ91 (GC) and shrinkage porosity and gas pores in the die cast material of AZ91 and AM50 (Figs. 7 and 8), while the hardness measurements and the bending tests provided values in a real scale. As a criterion for plastic deformation the bending angle shows the superiority of the AE-alloys.

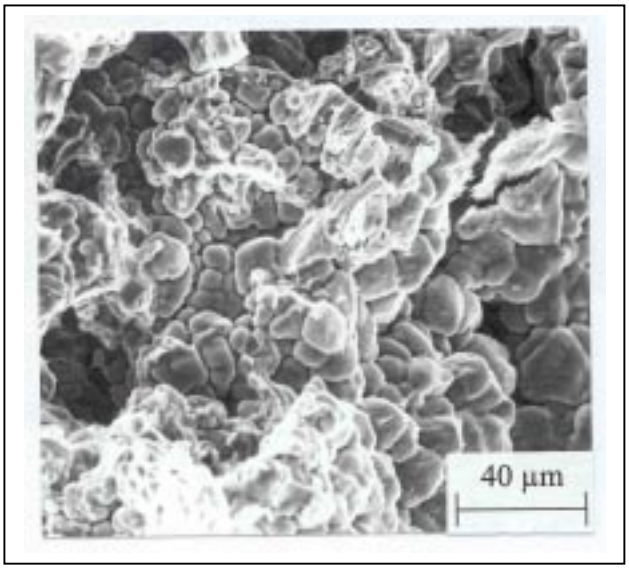

Figure 7: Shrinkage porosity on the fracture surface of AM 50 II (DC)

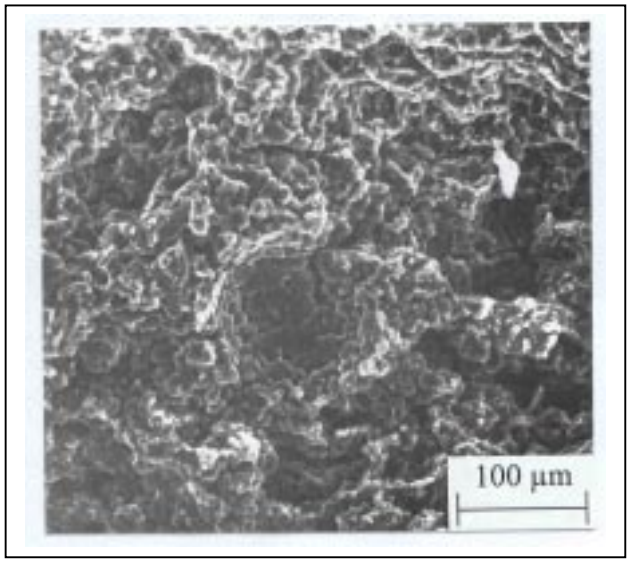

Figure 8: Gas pore with oxid layer on the fracture surface of AZ91 (DC)

The energy absorption capability of the different materials is characterized by the impact test response. The K-values determined on 5x10x55 mm plates (Table 2) seem to be able to separate the impact sensitivity of the investigated alloys with regard to their microstructure and castings defects, also in comparison with the fracture elongation data. From testing results of real Charpy specimens without notch and with a machined-in notch (Table 3) can be underlined the utility of a fitted impact test in quality control procedures of cast products.

Remarkable are the large differences between the two AM50 charges (Table 2) which cannot only result from the higher porosity in the AM50 II. To contribute to the explanation of this fact subsequent EDX-investigations were made. It was found that the Al-content with ≈ 7% was too high, near the composition of an AZ81. This explains the similarity of the data to that of AZ91. The casting of AM50 often occurs by mixing of AZ91 with AM20 to reduce the Al-content. For lack of carefullness could it be possible that such a component is subjected to impact loading.

TABLE 3
IMPACT TOUGHNESS AND FRACTURE TOUGHNESS

Alloy/ condition	K without notch [J]	KV2 [J]	K_{Fmax} [MPa $m^{½}$]			
			10x10 mm fatigue crack	3x6* mm sawing cut	3x6mm fatigue crack	10x5mm fatigue crack
AZ91 (GC)	3.4-6.8	2.4-2.6	12.9-14.5			11.8-13.5
AZ91 (DC)	1.4-4.8	0.8-1.2	7.7-12.6	10.1-14.0	7.1-11.7	8.2-9.6
AE42 (GC)	8.6-14.4	4.0-4.9	16.4-17.9			
AE42 (DC)	-	-	-	20.0	15.7-19.4	16.4-19.1
AM50 I(DC)	-	-	-	15.9-16.5		
AM50 II(DC)				7.2-9.9		

* Specimen width x specimen hight

The fracture mechanics tests were carried out in different ways. The loading occured both in a usual tensile-compression test machine and in a special bending stage as an additional equipment to the SEM allowing the direct observation of the damage process [11]. In the Table 3 are presented the obtained fracture toughness values calculated from F_{max} [12]. The differences in the fracture toughness reflect the distinction in the chemical composition, paticularly in the Al-content, and in the cast technology. To comment the influence of the fatigue crack or sawing cut on the test result the number of investigated specimens is still to low. It seems that a sawing cut necessary in small specimen leads to some higher fracture toughness values.
From the recorded load-deflection curves it was possible to conclude that a determination of fracture toughness by using of F_{max} in a linear-elastic manner underestimates the ductility of the most of the investigated alloys. Only the specimens from AZ91 (DC) and AM50 II (DC) failured by fracture. Therefore a comparison on specimens similar in the outside dimensions and the a_0/W- ratio was made to calculate the fracture toughness in formal accordance with fracture mechanics test standards [12,13] by different approaches. The results are listed in Table 4 for the pressure die cast materials. The both K_J-values are exchanged values from J-integral into K using for J_{ges} the complete work was done in the specimen and for $J_{el\,/\,pl}$ the plastic portion, only.

TABLE 4
FRACTURE TOUGHNESS USING DIFFERENT ASSESSMENTS

K in MPa $m^{½}$ alloy	K_{Fmax}	K_Q	$K_{J\,ges}$	$K_{J\,el\,/\,pl}$
AZ91 (DC)	10.0	7.6	17.1	15.4
AE42 (DC)	18.1	13.7	35.7	33.2
AM50 I (DC)	16.4	14.2	24.9	22.6
AM50 II (DC)	8.2	7.2	16.4	13.8

The use of an elastic-plastic approach seems to be better to qualify the different alloys with regard to their deformability and crack sensitivity. Therefore, in cases of the application of ingots as raw material and a thick-walled AZ91 pressure die casting precracked Charpy specimens were used to develop crack resistance curves J - Δa by application of the multispecimen test method (Fig. 9).

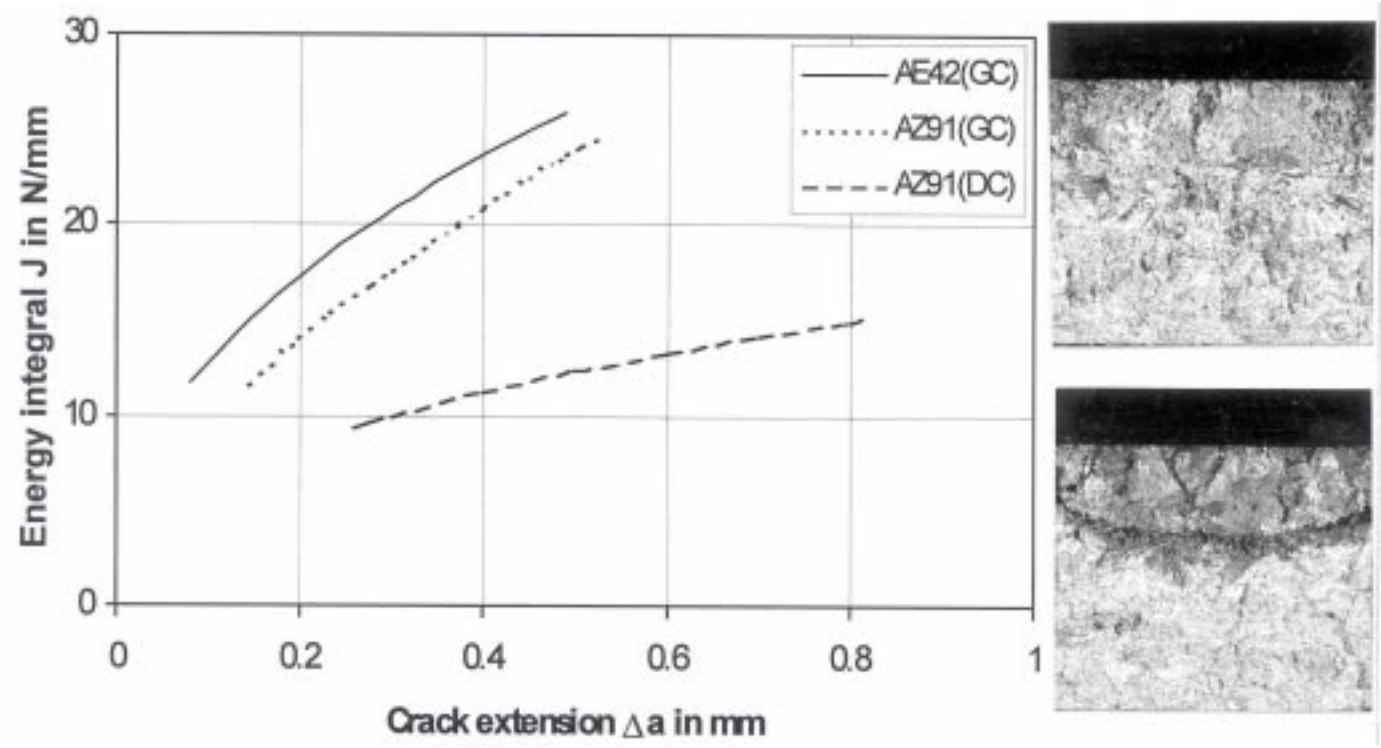

Figure 9: Crack resistance curves J - Δa and fracture surfaces of AE42 (GC)

Precracked specimen were loaded to different displacement levels and after unloading the amount of crack extension has to be marked. The heat tinting method, which on steels provides excellent results, was not successfull on magnesium alloys at different temperatures and furnace atmospheres. Therefore, the specimens were subjected to a second fatigue loading. Microscopically, the both fatigue fracture surfaces can be observed. However, an exact separation allowing the measurement of the stable crack growth Δa is not possible. Although the use of liquid penetrants is not recommended in the ASTM E1737 [13] blue and red crack penetrants oil based with magnetic particles had been tested. After spraying the specimens were dried at 80°C for several hours and broken. Like to see on the micrograph in Fig. 9 the red penetrant (upper image) gives no sufficient contrast on the fracture surface, whereas the blue suspension is characterized by excellent creep properties, but a bad drying behaviour. The short time for the second cyclic loading is time enough that the penetrant creeps in the growing fatigue crack (Fig. 9, under image). Resulting from the very large grains in the AE42-ingot, the fatigue crack surface is very rough. Maybe further tests with other fatigue loading parameters can contribute to change the appearance and the roughness of the fatigue crack areas.
From the experimentally determined J-Δa-curves in Fig. 9 can be seen that the crack resistance in the AZ91 (DC) is the lowest one. In a great number existing casting defects considerably reduce the crack resistance. In the opposite to the behaviour in the tensile test the AZ91 (GC) specimens show a rather high crack resistance. This is attributed to the inhomogeneity with regard to the matrix grain size and volume fraction, size and distribution of the brittle β-phase $Mg_{17}Al_{12}$. Fig. 10 illustrates the crack path within the micro-structure of AZ91 (GC). The propagating crack grows along grain boundaries covered with compact and discontinuously precipitated β-phase. In the alloy AE42 (GC) the precipitates form no chains or nets. Locally were found ring-shaped clusters of fine precipitates (Fig. 11). These are not artefacts from the preparation process, by TEM investigations can be lightened the character of the different particles, only. From the crack path in Fig. 11 is evident that the extension is primary controlled by the stress field on the crack tip. The initial crack as a fatigue crack or formed by precipitate debonding can blunt in the matrix and in this way a certain amount of energy is used for plastic deformation. Therefore, the alloy AE42 (DC) is characterized by a crack resistance curve with a rather high slope. Because the mentioned above problems to measure the stable crack length no results were get in the region of very small Δa-values. A stretched zone like in steels and in other materials was not found up to now. For this reason it is also impossible to define a criterion for a crack initiation toughness.

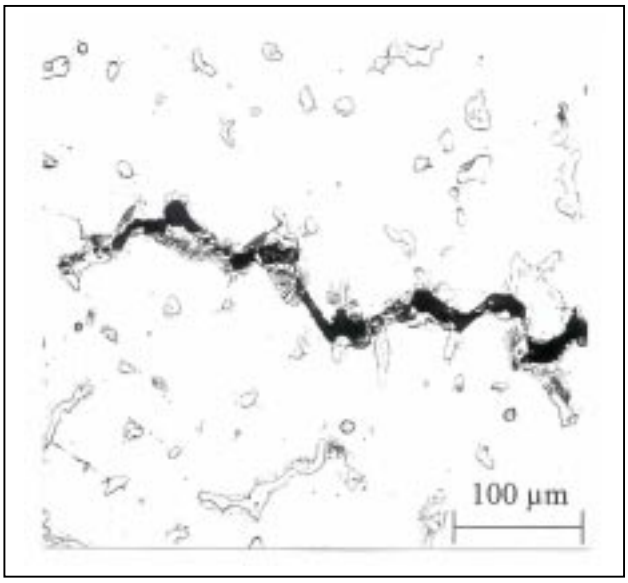

Figure 10: Crack path in AZ91 (GC) through $Mg_{17}Al_{12}$ - phase

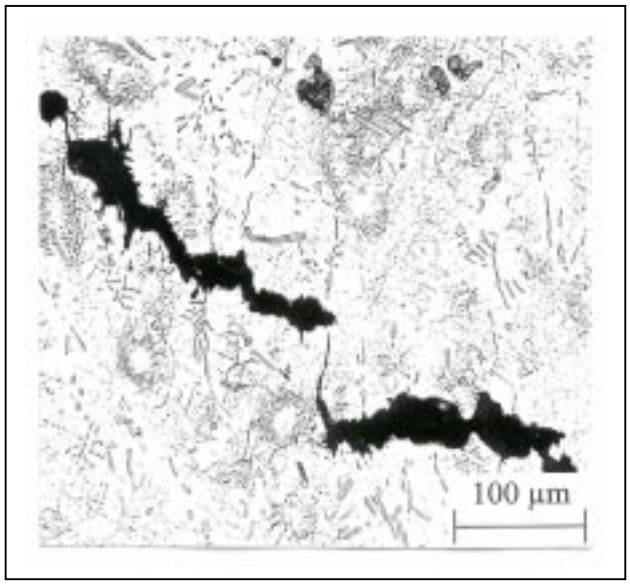

Figure 11: Crack path in AE42 (GC), void coalescence

CONCLUSIONS

1. Deviations in the chemical composition and in the casting technology of components lead to essential changes in the microstructure and consequently in the mechanical properties. Therefore, it is important to select the suitable alloy for a given component, to create a fitted technology and to guarantee the adherence of these requirements.

2. Impact tests on Charpy specimens or on a definite plate (with or without a notch in dependence on the material thickness) appear to be suitable to characterize the material and the casting. This specimens are smaller than tensile specimens, in the most cases to machine from a die casting and the test is not expensive.

3. From fracture mechanics testing can be concluded that the crack sensitivity is the lowest one in the AE42 both in the ingot and in the die cast component. The material damage starts at precipitates of the grain boundaries, frequently also by very large deformation in the matrix causing the formation of microcracks. Such a running crack can be retarded or arrested by blunting of the crack tip in the matrix.

4. With regard to the considerable plastic deformation in good quality alloys the application of elastic-plastic fracture mechanics is necessary to estimate the crack resistance. The multiple specimen method requires the development of a suitable marker technique to distinguish the regions of precrack and the stable crack growth on the fracture surfaces.

ACKNOWLEDGEMENT

The authors like to express their gratitude to the Kultusministerium des Landes Sachsen-Anhalt for financial support of this research work.

REFERENCES

[1] Aune,T.K., Westengen, H. and Ruden, Th. (1993). *SAE Technical Paper* Series 930418, 51-57.
[2] King, J.F. (1998). In: *Magnesium Alloys and their Applications*, 247-252. Mordike, B.L. and Kainer, K.U. (Eds). DGM Informationsges. mbH, Frankfurt.
[3] Tikal, F., Vollmer, C. and Zeißler, M. (1997) *Mat.-wiss. und Werkstofftechn*. **28**, 276-279.
[4] Schaberger, E., Kahn, D. and Lang, M. (1998) *Prakt.Metallogr*. **35**, 306-315.
[5] Schick, E. and Regener, D. (2000) *Prakt. Metallogr*. **37,** in press.
[6] Aghion, E. and Bronfin, B. (1998). In: *Magnesium Alloys and their Applications,* 295-300. Mordike, B.L. and Kainer, K.U. (Eds). DGM Informationsges. mbH, Frankfurt.
[7] Dargusch, M., Hisa, M., Caceres, C. H. and Dunlop, G. L.(1996). In: *Proc. of the 3. Int. Magnesium Conf.,* Manchester, 153-165. Lorimer, G.W. (Ed.). The University Press, Cambridge.
[8] Pettersen, G., Westengen, H., Hoier, R. and Lohne, O. (1996) *Material Science and Engineering* **A 207,** 115-120.
[9] Regener, D., Wagner, I., Schick, E. and Heyse, H. (1999) *Gießerei-Forschung* **51**, 154-160.
[10] Schindelbacher, G. and Rösch, R. (1998). In: *Magnesium Alloys and their Applications,* 247-252. Mordike, B.L. and Kainer, K.U. (Eds). DGM Informationsges. mbH, Frankfurt.
[11] Regener, D., Schick, E. and Wagner, I. (1999). In: *Bruchmechanische Konzepte im Leichtbau.* DVM-Bericht 231 307-316.
[12] Metallic materials – Determination of plane-strain fracture toughness. ISO 12737:1996.
[13] Standard test method for J-integral characterization of fracture toughness. ASTM E 1737 – 96.